

Accurate pulsar timing array residual variances and correlation of the stochastic gravitational wave background

Reginald Christian Bernardo^{1,*} and Kin-Wang Ng^{2,3,†}

¹*Asia Pacific Center for Theoretical Physics, Pohang 37673, Korea*

²*Institute of Physics, Academia Sinica, Taipei 11529, Taiwan*

³*Institute of Astronomy and Astrophysics, Academia Sinica, Taipei 11529, Taiwan*

Pulsar timing arrays have reported a compelling evidence of a nanohertz stochastic gravitational wave background. However, the origin of the signal remains undetermined, largely because its spectrum is bluer for an astrophysical source and can be explained by cosmological models. In this letter, we derive theoretically accurate expressions for the Fourier bin variances and correlation of pulsar timing residuals, and demonstrate their outstanding agreement with astrophysical simulations. In contrast, we show that a common power law traditionally used to interpret a stochastic gravitational wave background spectrum is generally faced with systematic errors, one of which is the illusion of a bluer signal. This hints at a conservative solution, supportive of an astrophysical source, to the observed correlated common spectrum process in pulsar timing arrays.

Pulsar timing array (PTA) collaborations have provided evidence of a correlated common spectrum process across Galactic millisecond pulsars, consistent with a stochastic gravitational wave background (SGWB) in the nanohertz regime [1–4]. This signal is characterized by a quadrupolar correlation matching the long-sought Hellings & Downs (HD) curve [5]. However, the constrained spectrum appears bluer than expected compared with the conservative supermassive black hole binaries (SMBHB) model, sparking a tantalizing debate about the origin of the signal [6–14].

This situation has propelled the field in several directions. One possibility is that current PTA data may be insufficient to definitively distinguish between various potential astrophysical and cosmological sources, suggesting that stronger constraints might emerge only with future data [15, 16]. Alternatively, we can explore new theoretical aspects, such as cosmic variance [17, 18], or observational techniques like analyzing the cumulants of the spectrum [19] and correlation [20], to fully leverage the capability of PTAs in constraining physical models.

Now is also an opportune time to revisit the foundational elements of both theory and PTA data analysis, addressing any systematic errors that could obscure or exaggerate the detection of a SGWB signal [21]. This letter is geared toward this direction—reexamining the interpretation of a SGWB signal through the Fourier modes of the PTA timing residuals, leading to new accurate expressions for the residuals’ bin variances and correlation (8–11). The new expressions turns out to be remarkably consistent with astrophysical simulations [22]. Most importantly, this reexamination has brought to light facets of the standard analysis that reflect as systematic errors on an inferred SGWB spectrum, such as biasing a spectrum to the blue side (Table I).

This letter proceeds with a derivation of theoretically

accurate PTA residual variances and correlation due to a SGWB, followed by a rigorous comparison with simulations. We use units $G = c = 1$, subscripts a, b to denote pulsars, and j, k for frequency bins.

In practice, the pulsar timing residual is expanded as a Fourier series [23],

$$r(t, \hat{e}) = \frac{\alpha_0(\hat{e})}{2} + \sum_{k=1}^{\infty} \alpha_k(\hat{e}) \sin(\omega_k t) + \sum_{k=1}^{\infty} \beta_k(\hat{e}) \cos(\omega_k t), \quad (1)$$

where $\omega_k = 2\pi f_k$, $f_k = k/T$, k is a positive integer, T is the total observation time, and \hat{e} is a pulsar direction unit vector¹. For brevity, we write down $\langle X_{aj} Y_{bk} \rangle \equiv \langle X_j(\hat{e}_a) Y_k(\hat{e}_b) \rangle$ where $X_j(\hat{e}_a)$ and $Y_k(\hat{e}_b)$ represent either one of the timing residual’s Fourier components $\alpha_j(\hat{e}_a)$ and $\beta_k(\hat{e}_b)$. Then, for the GWB part, it is taken that [24, 25]

$$\begin{aligned} \langle \alpha_{aj} \alpha_{bk} \rangle &\propto I(f_k) \gamma^{\text{HD}}(\hat{e}_a \cdot \hat{e}_b) \delta_{jk}, \\ \langle \beta_{aj} \beta_{bk} \rangle &\propto I(f_k) \gamma^{\text{HD}}(\hat{e}_a \cdot \hat{e}_b) \delta_{jk}, \\ \langle \alpha_{aj} \beta_{bk} \rangle &= 0, \end{aligned} \quad (2)$$

where $\gamma^{\text{HD}}(\hat{e}_a \cdot \hat{e}_b)$ is the HD curve, $I(f)$ is the SGWB power spectrum, and $\langle \dots \rangle$ denote ensemble averaging. If $T \sim 1$ yr, then the fundamental frequency is $f_1 \sim 31.8$ nHz; if $T \sim 15$ yr, then $f_1 \sim 2.1$ nHz. Following this logic, PTAs are able to measure the power spectrum at lower frequencies, $\sim I(1/T)$, through longer observing periods and increasing sky coverage. The Kronecker delta, δ_{kj} , can be read as an extremely localized filter at frequencies $\sim f_k$, giving PTAs source information at infinitesimally narrow bins.

In the following, we shall derive accurate PTA residual variances and correlation, as opposed to the highly idealized (2).

¹ The Fourier components of the timing residual are given by $\alpha_0(\hat{e}) = (2/T) \int_0^T dt r(t, \hat{e})$, $\alpha_i(\hat{e}) = (2/T) \int_0^T dt r(t, \hat{e}) \sin(\omega_i t)$, and $\beta_i(\hat{e}) = (2/T) \int_0^T dt r(t, \hat{e}) \cos(\omega_i t)$.

* reginald.bernardo@apctp.org

† nk@phys.sinica.edu.tw

Consider an isotropic and Gaussian SGWB. In symbols, we write down

$$\langle h_A(f, \hat{k}) h_{A'}^*(f', \hat{k}') \rangle = \delta_{AA'} \delta(f - f') \delta(\hat{k} - \hat{k}') I(f), \quad (3)$$

where $h_A(f, \hat{k})$ are GW amplitudes. For simplicity, we consider equidistant pulsars relative to Earth, $D_a \sim D_b \sim D \sim 1$ kpc. Then, the timing residual cross correlation can be written as [26–28]

$$\langle r(t_1, \hat{e}_a) r(t_2, \hat{e}_b) \rangle = \int_0^\infty \frac{2df}{(2\pi f)^2} I(f) \gamma(fD, \hat{e}_a \cdot \hat{e}_b) C(f, t_1, t_2), \quad (4)$$

where $\gamma(fD, \hat{e}_a \cdot \hat{e}_b)$ is the spatial correlation, and

$$C(f, t_1, t_2) = 1 - \cos(2\pi f t_1) - \cos(2\pi f t_2) + \cos[2\pi f(t_2 - t_1)] \quad (5)$$

is a temporal correlation owed to wave propagation in time. The spatial correlation can be written as

$$\gamma(fD, \hat{e}_a \cdot \hat{e}_b) = \sum_{l \geq 2} \frac{2l+1}{4\pi} C_l(fD) P_l(\hat{e}_a \cdot \hat{e}_b), \quad (6)$$

where the angular power spectrum, $C_l(y)$'s, is given by

$$C_l(y) = 2\pi^{3/2} \frac{(l+2)!}{(l-2)!} \left| \int_0^{2\pi y} dx e^{ix} \frac{j_l(x)}{x^2} \right|^2. \quad (7)$$

Note that the finite upper limit to the integral corresponds to the pulsar term. When dropped, $fD \gg 1$, as in Galactic millisecond pulsars and nanohertz frequencies, the $C_l(y)$'s reduce to the HD correlation power spectrum, $C_l(\infty) \sim C_l^{\text{HD}} = 8\pi^{3/2} / ((l-1)l(l+1)(l+2))$; in real space, the sum (6) can be analytically closed to give rise to the HD curve, $\gamma^{\text{HD}}(\hat{e}_a \cdot \hat{e}_b) = \gamma(\infty, \hat{e}_a \cdot \hat{e}_b)$.

The standard interpretation (2) is recovered by taking the equal time correlation, $t_1 = t_2 = t$, in (4) and dropping the factor $\sin^2(\pi f t)$. We shall show that dropping this frequency modulating factor has unintended consequences for parameter estimation.

In fact, using (4), it can be shown that *all* the correlation components across frequency bins can be compactly expressed as

$$\langle X_{aj} Y_{bk} \rangle = \mathcal{F}[I(f), \gamma(fD, \hat{e}_a \cdot \hat{e}_b), \mathcal{C}_{jk}^{(XY)}(f)], \quad (8)$$

where the functional \mathcal{F} is given by

$$\mathcal{F}[I(f), \gamma(fD, x), \mathcal{C}(f)] = \int_0^\infty \frac{2df}{(2\pi f)^2} I(f) \gamma(fD, x) \mathcal{C}(f), \quad (9)$$

and $\mathcal{C}_{jk}^{(XY)}(f)$ are filters specific to every component of the correlation². For us, the relevant ones can be teased

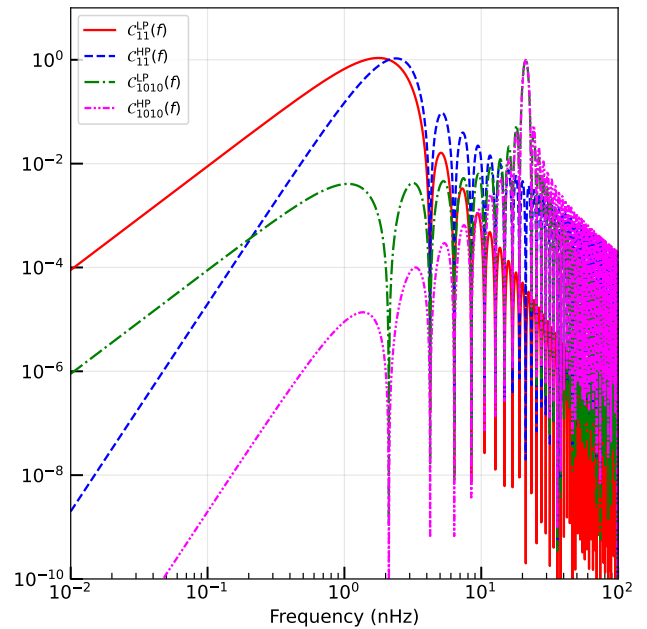


FIG. 1. Low-pass and high-pass frequency filters (10) and (11) in the 1st and 10th frequency bins with $T = 15$ yr; $f_1 \sim 2$ nHz, $f_{10} = 10f_1 \sim 20$ nHz.

out analytically,

$$\mathcal{C}_{jk}^{\text{LP}}(f) = \frac{4kj \sin^2(\pi f T)}{\pi^2 (k^2 - f^2 T^2) (j^2 - f^2 T^2)}, \quad (10)$$

and

$$\mathcal{C}_{jk}^{\text{HP}}(f) = \frac{4f^2 T^2 \sin^2(\pi f T)}{\pi^2 (k^2 - f^2 T^2) (j^2 - f^2 T^2)}, \quad (11)$$

which are the filters for $\langle \alpha_{aj} \alpha_{bk} \rangle$ and $\langle \beta_{aj} \beta_{bk} \rangle$, respectively. The relation $\mathcal{C}_{kj}^{\text{LP}}(f) / \mathcal{C}_{kj}^{\text{HP}}(f) \sim f^{-2}$ motivates us to refer to $\mathcal{C}_{kj}^{\text{LP}}(f)$ and $\mathcal{C}_{kj}^{\text{HP}}(f)$ as low-pass and high-pass filters, respectively. These are shown in Figure 1. The above expressions can be used to similarly show that the α - and β -bins, $\langle \alpha_{aj} \beta_{bk} \rangle$, are uncorrelated and different frequency bins ($k \neq j$) are very weakly correlated.

To show that the above formalism is robust, we turn to SGWB simulations in PTA using the standard `TEMPO2` [22, 30] timing software and its python wrapper `libstempo`³. We take the Meerkat PTA's 78 millisecond pulsars [29] as reference positions on the sphere (Figure 2), and simulate 15-year PTA mock data with input GWs at frequencies $f \in (1, 100)$ nHz from $\mathcal{O}(10^3)$ SMBHBs, a strain amplitude $A_{\text{gw}} = 2.4 \times 10^{-15}$, and a spectral index $\gamma_{\text{gw}} = 13/3$. We emphasize that our results hold irrespective of the arbitrary reference to Meerkat PTA pulsars. The sample variances of the

² The timing residual correlation and its Fourier components can be read as a convolution between the power spectrum, the spatial correlation, and a filter.

³ <https://github.com/vallis/libstempo>

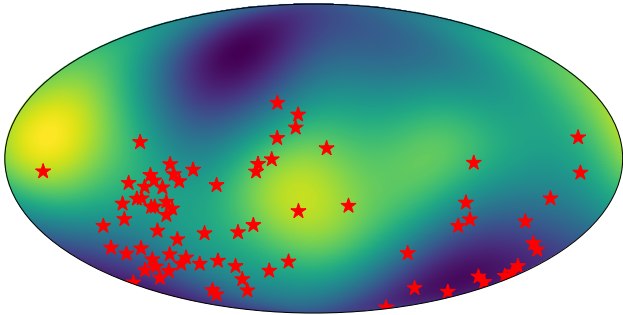


FIG. 2. Sky positions of the Meerkat PTA pulsars (red stars) [29] with a smoothed projection/map of a SGWB.

α - and β -bins are measured, and the ensemble statistics/cosmic variance is accounted for by repeating the simulation numerous times. We then use a Markov chain Monte Carlo (MCMC) approach to compare the bin variances of the mock data, $\langle \alpha_k^2 \rangle_{\text{sims}}$ and $\langle \beta_k^2 \rangle_{\text{sims}}$, to models based on (8-11) with power spectrum models $I_{M_0}(f) = I_{\text{ref}} \bar{f}^{-7/3}$ and $I_{M_1}(f) = I_{\text{ref}} \bar{f}^{2-\gamma}$ where $\bar{f} = f/(1 \text{ nHz})^4$. Because different frequency bins are practically uncorrelated, we consider a likelihood \mathcal{L} given by $\log \mathcal{L} \sim -0.5 \sum_k ((W_{k,M} - \bar{W}_{k,\text{sims}})/\Delta W_{k,\text{sims}})^2$ where $W_{k,M}$ and $W_{k,\text{sims}}$ are timing residual bin variances predicted by the model and of the mock data, respectively.

The constraints are shown in Figure 3, and the corresponding best fits to the bin variances and the correlation are shown in Figures 4-5, demonstrating excellent performance by the model. The takeaway is that the accurate (8-11) with a power law spectrum is naturally able to recover the precise spectral tilt, $\gamma \sim \gamma_{\text{gw}} = 13/3$, expected of a SGWB from a myriad of SMBHBs. Notably, both one- and two-parameter models, M_0 and M_1 , are consistent with inferring the power spectrum's reference value, I_{ref} . This consistency between the two models can also be seen in the best fit bin variances and correlation, as shown in Figures 4-5. The correlation is in tune with the HD curve, indicative of a gravitational wave signal. It is worth highlighting that the choice of reference frequency is immaterial, i.e., any choice gives the same posterior, with appropriately shifted amplitude⁵.

However, a main point of this letter emerges illustratively through the bin variances inferred by the usual common power law (cpl), $I_{\text{cpl}}(f) = I_{\text{ref}} \bar{f}^{2-\gamma}$, anchored on (2) that is fitted to both α - and β -bin variances. This is shown in Figure 4, when the cpl spectral index γ is varied in $\gamma \in (2.3, 4.3)$. A cpl based on (2) fitted to both α - and β -bin variances always infers a bluer spectrum

⁴ I_{ref} is the power spectrum at a frequency $\sim 1 \text{ nHz}$.

⁵ If $f_{\text{ref}} \rightarrow f'_{\text{ref}}$, then $I'_{\text{ref}} = I_{\text{ref}} (f'_{\text{ref}}/f_{\text{ref}})^{2-\gamma}$.

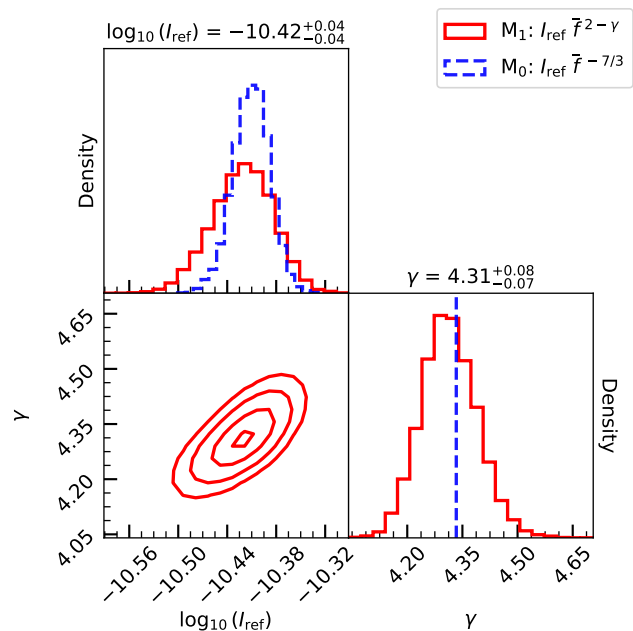


FIG. 3. Constraints on the power spectrum models $I_{M_0}(f) = I_{\text{ref}} \bar{f}^{-7/3}$ and $I_{M_1}(f) = I_{\text{ref}} \bar{f}^{2-\gamma}$ with accurate bin variances (8-11) using 15-yr Meerkat PTA mock data with input GWs at frequencies $f \in (1, 100) \text{ nHz}$ from $\mathcal{O}(10^3)$ SMBHBs, $A_{\text{gw}} = 2.4 \times 10^{-15}$, and $\gamma_{\text{gw}} = 13/3$.

TABLE I. Constraints on the power spectrum $I(f)$ using the standard analysis ((2)+cpl) and this work ((8-11)+ M_1) given TEMPO2 simulated 15-yr Meerkat PTA data with input GWs at frequencies $f \in (1, 100) \text{ nHz}$ from $\mathcal{O}(10^3)$ SMBHBs, $A_{\text{gw}} = 2.4 \times 10^{-15}$, and $\gamma_{\text{gw}} = 13/3$.

Model	Noise (μs^2)	$\log_{10}(I_{\text{ref}})$	γ
(2)+cpl	0	$-10.33^{+0.06}_{-0.07}$	$4.22^{+0.08}_{-0.09}$
	10^{-3}	$-10.5^{+0.1}_{-2.2}$	$3.9^{+0.4}_{-3.9}$
	10^{-2}	$-10.6^{+0.2}_{-0.7}$	$3.0^{+0.9}_{-2.2}$
(8-11)+ M_1	0	-10.42 ± 0.04	$4.31^{+0.08}_{-0.07}$
	10^{-3}	$-10.42^{+0.04}_{-0.05}$	4.2 ± 0.2
	10^{-2}	-10.4 ± 0.1	$4.5^{+0.9}_{-0.5}$

contrary to the expectation; for the SMBHB spectrum, cpl turns in $7/3 \lesssim \gamma \lesssim 13/3$. In addition to the spectral index, a cpl based on (2) is likely to output a systematic error to the inferred amplitude of the spectrum because of the power difference between the α - and β -bins. This turns out to be less of an issue after fitting the timing model and considering one-point noise, roughly equalizing the power between bins. A systematic error and dependence on the reference frequency of the amplitude will persist if the data is sufficiently precise.

Elaborating on the pitfalls of associating the bin variances with (2) and a cpl, we consider different levels of one-point noise, emphasizing that the bin variances are one-point measures of the signal. The constraints are

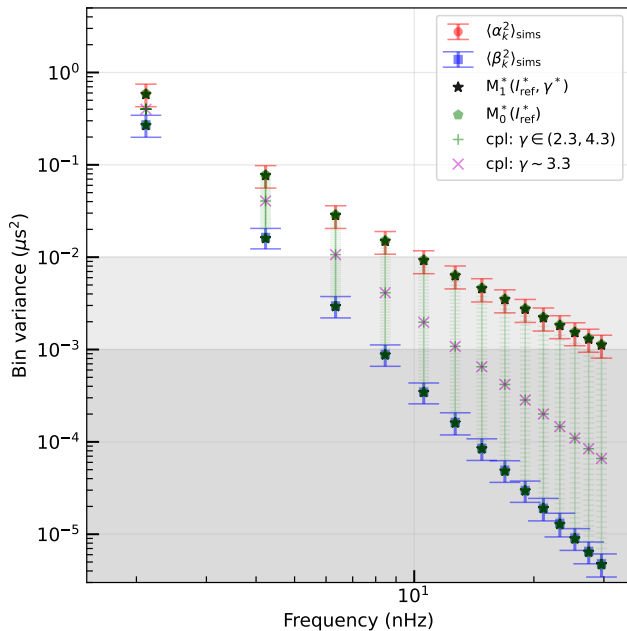


FIG. 4. Simulated bin variances in 15-yr MeerKAT PTA mock data (red and blue points/error bars) with input GWs at frequencies $f \in (1, 100)$ nHz from $\mathcal{O}(10^3)$ SMBHBs, $A_{\text{gw}} = 2.4 \times 10^{-15}$, and $\gamma_{\text{gw}} = 13/3$. Black stars and green pentagons are best fits from models $M_1^+(I_{\text{ref}}^*, \eta^*)$ and $M_0^+(I_{\text{ref}}^*)$, respectively, and (8-11). Violet ‘x’ and green ‘+’ are bin variances corresponding to a common power law model saturated to fit both α - and β -bin variances of the mock data. Shaded regions below thresholds $\sim 10^{-3} \mu\text{s}^2$ and $\sim 10^{-2} \mu\text{s}^2$ depict typical one-point noise levels.

shown in Table I. In the noise-free case, depicted by the red and green points in Figure 4, a cpl turns out to be able to infer the SMBHB spectrum, but only by happenstance since the β -bins have more weight in the likelihood due to their smaller uncertainty compared to the α -bins. It is notable that the noise-free case hints at a systematically bluer spectrum at 68% confidence compared to the expected SMBHB spectrum. This systematic error is exacerbated by any level of one-point noise. At $\sim 10^{-3} \mu\text{s}^2$, disabling the sensitivity to β -bins for $f \gtrsim 10$ nHz, a cpl infers $\log_{10}(I_{\text{ref}}) = -10.5_{-2.2}^{+0.1}$ and $\gamma = 3.9_{-3.9}^{+0.4}$. With noise at $\sim 10^{-2} \mu\text{s}^2$, the inferred parameters are $\log_{10}(I_{\text{ref}}) = -10.6_{-0.7}^{+0.2}$ and $\gamma = 3.0_{-2.2}^{+0.9}$. Accordingly, the posterior of the amplitude and the spectral index becomes bimodal, reaching local maxima at the α - and β -bins because (2) and cpl is saturated to fit two different spectra. Undesirably, a blue-tilted spectrum compared to SMBHB is always inferred by the standard analysis with a cpl.

In contrast, the same typical one-point noise levels do not lead to analogous systematic error contamination when using the accurate expressions (8-11), showcasing its robustness in modelling the bin-variances of a SGWB in a PTA. Table I clearly shows this. The inferred parameter posteriors are consistent with each other and the

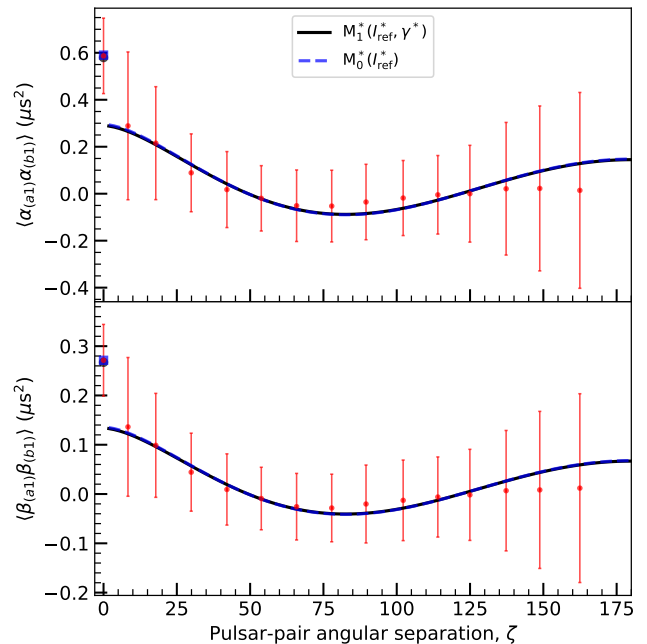


FIG. 5. Correlation in the 1st frequency bin, $f_1 \sim 2$ nHz, in 15-yr MeerKAT PTA mock data (red points/error bars) with input GWs at frequencies $f \in (1, 100)$ nHz from $\mathcal{O}(10^3)$ SMBHBs, $A_{\text{gw}} = 2.4 \times 10^{-15}$, and $\gamma_{\text{gw}} = 13/3$. Black-solid and blue-dashed lines show the best fits $M_1^+(I_{\text{ref}}^*, \eta^*)$ and $M_0^+(I_{\text{ref}}^*)$, respectively.

expected values, only statistically wider depending on the amount of one-point noise.

It is worth mentioning that our analysis could also easily be extended to post-fit residuals, in which case the power spectrum in (8-11) must be changed to $I(f)\mathcal{T}(f)$ where $\mathcal{T}(f)$ is the transmission function [31]. In this case, the power below the fundamental frequency, $f \lesssim 1/T$, and the power difference between the α - and β -bins can be expected to drop, but the spectrum will remain intact up to $\mathcal{O}(10^2)$ nHz. In the end, the conclusions would be the same.

We highlight the important roles of the temporal correlation (5), and the corresponding filters (10-11), in our analysis, which we deem are as profound as the HD curve for recognizing a SGWB signal. In this letter, we have shown that PTA residual variances and correlation based on (8-11) align perfectly with simulated signal from SMBHBs. Naturally, the accuracy of the expressions used for interpretation must meet the precision of the data in order to extract meaningful insights. Our results have shown that the standard common power law and (2) used to interpret a SGWB signal inevitably introduce systematic errors in the inferred spectrum (Table I). More sophisticated models may undeniably be able to get away with a better fit, but this would not help out in the physical interpretation of the signal. Ultimately, the SGWB piece of the covariance of the PTA likelihood must be updated according to (8-11) to properly account for these

systematic biases when analyzing the data. This shows that an inferred bluer signal can be a byproduct of such systematics and potentially hints at a conservative solution to the debated source of the PTA signal, tracing it to astrophysics.

The authors thank Achamveedu Gopakumar, Subhajit Dandapat, and Debabrata Deb for relevant discussion on PTA simulations. RCB is supported by an appointment

to the JRG Program at the APCTP through the Science and Technology Promotion Fund and Lottery Fund of the Korean Government, and was also supported by the Korean Local Governments in Gyeongsangbuk-do Province and Pohang City. This work was supported in part by the National Science and Technology Council of Taiwan, Republic of China, under Grant No. NSTC 113-2112-M-001-033.

-
- [1] G. Agazie *et al.* (NANOGrav), *Astrophys. J. Lett.* **951**, L8 (2023), arXiv:2306.16213 [astro-ph.HE].
 - [2] D. J. Reardon *et al.*, *Astrophys. J. Lett.* **951**, L6 (2023), arXiv:2306.16215 [astro-ph.HE].
 - [3] J. Antoniadis *et al.* (EPTA, InPTA:), *Astron. Astrophys.* **678**, A50 (2023), arXiv:2306.16214 [astro-ph.HE].
 - [4] H. Xu *et al.*, *Res. Astron. Astrophys.* **23**, 075024 (2023), arXiv:2306.16216 [astro-ph.HE].
 - [5] R. W. Hellings and G. W. Downs, *Astrophys. J. Lett.* **265**, L39 (1983).
 - [6] E. S. Phinney, (2001), arXiv:astro-ph/0108028.
 - [7] A. Sesana, F. Haardt, P. Madau, and M. Volonteri, *Astrophys. J.* **611**, 623 (2004), arXiv:astro-ph/0401543.
 - [8] J. Antoniadis *et al.* (EPTA), (2023), arXiv:2306.16227 [astro-ph.CO].
 - [9] A. Afzal *et al.* (NANOGrav), *Astrophys. J. Lett.* **951**, L11 (2023), arXiv:2306.16219 [astro-ph.HE].
 - [10] Y.-M. Wu, Z.-C. Chen, and Q.-G. Huang, *Sci. China Phys. Mech. Astron.* **67**, 240412 (2024), arXiv:2307.03141 [astro-ph.CO].
 - [11] J. Ellis, M. Fairbairn, G. Franciolini, G. Hütsi, A. Iovino, M. Lewicki, M. Raidal, J. Urrutia, V. Vaskonen, and H. Veermäe, *Phys. Rev. D* **109**, 023522 (2024), arXiv:2308.08546 [astro-ph.CO].
 - [12] L. Bian, S. Ge, J. Shu, B. Wang, X.-Y. Yang, and J. Zong, *Phys. Rev. D* **109**, L101301 (2024), arXiv:2307.02376 [astro-ph.HE].
 - [13] Y.-C. Bi, Y.-M. Wu, Z.-C. Chen, and Q.-G. Huang, *Sci. China Phys. Mech. Astron.* **66**, 120402 (2023), arXiv:2307.00722 [astro-ph.CO].
 - [14] J. P. W. Verbiest, S. J. Vigeland, N. K. Porayko, S. Chen, and D. J. Reardon, *Results Phys.* **61**, 107719 (2024), arXiv:2404.19529 [astro-ph.HE].
 - [15] T. J. W. Lazio, *Class. Quant. Grav.* **30**, 224011 (2013).
 - [16] A. Weltman *et al.*, *Publ. Astron. Soc. Austral.* **37**, e002 (2020), arXiv:1810.02680 [astro-ph.CO].
 - [17] B. Allen, *Phys. Rev. D* **107**, 043018 (2023), arXiv:2205.05637 [gr-qc].
 - [18] R. C. Bernardo and K.-W. Ng, *JCAP* **11**, 046 (2022), arXiv:2209.14834 [gr-qc].
 - [19] W. G. Lamb and S. R. Taylor, *Astrophys. J. Lett.* **971**, L10 (2024), arXiv:2407.06270 [gr-qc].
 - [20] R. C. Bernardo, S. Appleby, and K.-W. Ng, (2024), arXiv:2407.17987 [astro-ph.CO].
 - [21] V. Di Marco, A. Zic, R. M. Shannon, and E. Thrane, *Mon. Not. Roy. Astron. Soc.* **532**, 4026 (2024), arXiv:2403.13175 [astro-ph.HE].
 - [22] G. Hobbs, F. Jenet, K. J. Lee, J. P. W. Verbiest, D. Yardley, R. Manchester, A. Lommen, W. Coles, R. Edwards, and C. Shettigara, *Mon. Not. Roy. Astron. Soc.* **394**, 1945 (2009), arXiv:0901.0592 [astro-ph.SR].
 - [23] S. R. Taylor, (2021), arXiv:2105.13270 [astro-ph.HE].
 - [24] A. D. Johnson *et al.* (NANOGrav), *Phys. Rev. D* **109**, 103012 (2024), arXiv:2306.16223 [astro-ph.HE].
 - [25] G. Agazie *et al.*, (2024), arXiv:2407.20510 [astro-ph.HE].
 - [26] G.-C. Liu and K.-W. Ng, *Phys. Rev. D* **106**, 064004 (2022), arXiv:2201.06767 [gr-qc].
 - [27] R. C. Bernardo and K.-W. Ng, *Phys. Rev. D* **107**, 044007 (2023), arXiv:2208.12538 [gr-qc].
 - [28] P. F. Depta, V. Domcke, G. Franciolini, and M. Pieroni, (2024), arXiv:2407.14460 [astro-ph.CO].
 - [29] M. T. Miles *et al.*, *Mon. Not. Roy. Astron. Soc.* **519**, 3976 (2023), arXiv:2212.04648 [astro-ph.HE].
 - [30] G. Hobbs, R. Edwards, and R. Manchester, *Mon. Not. Roy. Astron. Soc.* **369**, 655 (2006), arXiv:astro-ph/0603381.
 - [31] J. S. Hazboun, J. D. Romano, and T. L. Smith, *Phys. Rev. D* **100**, 104028 (2019), arXiv:1907.04341 [gr-qc].